



# OPEN Long-term exposure to PM<sub>2.5</sub> exacerbates dopaminergic neuronal loss through CpG hypermethylation induced down-regulation of PINK1 and DJ-1 genes

Xiangnan Du<sup>1</sup>, Longfei Guan<sup>2</sup>, Chen Chen<sup>2</sup>, Xuemei Wang<sup>1</sup>✉ & Xiaokun Geng<sup>1,2</sup>✉

To investigate whether airborne particle (PM<sub>2.5</sub>) aggravates Parkinson's disease (PD) and alter expression of key PD-related genes by DNA methylation. Two groups of rats were exposed to either clean air or polluted air for 3, 6, and 12 months. The neurotoxin rotenone was injected intraperitoneally to induce a Parkinson's-like disorder. Immunostaining was used to measure the number of dopaminergic neurons in substantia nigra (SN). Real-time PCR was used to measure mRNA levels of PD-related genes *PINK1* and *DJ-1* in SN. Bisulfate sequencing (BSP) was used to measure DNA methylation levels in gene promoters. In a cell-based mimic of animal experiments, SH-SY5Y cells were treated with Diesel exhaust PM<sub>2.5</sub> (DEP) for 1.5, 6, and 24 h. RT-PCR and BSP methods were used to measure gene expression and methylation of CpG islands in the cells. Persistent exposure to PM<sub>2.5</sub> significantly increased the loss of dopaminergic neurons in the SN. Prolonged PM<sub>2.5</sub> exposure and DEP treatment significantly reduced the mRNA levels of *PINK1* and *DJ-1*. Both PM<sub>2.5</sub> and DEP significantly increased the methylation level of the CpG islands in both genes. PM<sub>2.5</sub> induced loss of dopaminergic neurons and aggravated Parkinson's disease. PM<sub>2.5</sub> induced dysregulation of DNA methylation, resulting in decreased expression of the *PINK1* and *DJ-1*.

**Keywords** Parkinson's disease, PM<sub>2.5</sub>, *PINK1*, *DJ-1*, CpG hypermethylation

Parkinson's disease (PD) is one of the most common neurodegenerative diseases worldwide, second only to Alzheimer's disease. The incidence, which increases with age, is 1–2% in the population over 65-year-old and 4% for people over 85-year-old<sup>1</sup>. With rising population, China has entered an aging society, and the morbidity of PD will increase constantly and undoubtedly be a serious burden to the economy. However, the pathogenesis of PD is not completely clear.

Fine particulate matter (PM<sub>2.5</sub>) is the main pollutant that causes haze weather. With the rapid development of the economy, haze pollution has gradually developed into a prominent environmental problem in China. However, it was not until recently that people realized the seriousness of PM<sub>2.5</sub> pollution. Animal trials indicate that the olfactory mucosa may be an entry route for air pollutants to disturb the blood–brain barrier and negatively affect the central nervous system (CNS)<sup>2,3</sup>. Considerable evidence supports a link between PM<sub>2.5</sub> exposure and the development of CNS diseases, including PD and other neurodegenerative diseases<sup>4–8</sup>. Wang's study showed that exposure to PM<sub>2.5</sub> aggravated the symptom of PD in rotenone-treated mouse by inducing the dysfunction of mitochondria and *PINK1*/*Parkin* signaling pathways were involved in the aggravative effects of PM<sub>2.5</sub><sup>9</sup>. In addition, both Zanobetti's and Hyewon Lee's research indicated that PD patients required hospitalization after short-term exposure to elevated PM<sub>2.5</sub> levels<sup>10,11</sup>.

Various PD-related genes have been identified, and knowledge about the genetics of PD has exploded<sup>12</sup>. The first gene associated with PD was identified in 1997 as a missense mutation in the *α-synuclein* (*SNCA*) gene; the gene is regulated by DNA methylation and the missense mutation increases the risk of PD<sup>13</sup>. The phosphatase and tensin homologue-induced putative kinase 1 gene (*PINK1*)<sup>14</sup> and the *DJ-1* gene<sup>15</sup> are also closely related to the pathogenesis of PD. The *PINK1* and *DJ-1* genes<sup>16</sup> protect mitochondrial from oxidative stress, and their

<sup>1</sup>Department of Neurology, Beijing Luhe Hospital, Capital Medical University, 82# South of Xin Hua, Beijing 101100, China. <sup>2</sup>Department of Neurology, China-America Institute of Neuroscience, Beijing Luhe Hospital, Capital Medical University, 82# South of Xin Hua, Beijing 101100, China. ✉email: shining0881@sina.com; xgeng@ccmu.edu.cn

downregulation aggravates the oxidative stress response and promote apoptosis. The *DJ-1* gene can be regulated by DNA methylation. DNA methylation, a common type of epigenetic modification, has an important function in the pathogenesis of PD. DNA methylation can silence gene expression, thereby reducing the protective effects of genes and promoting the progress of PD. Nevertheless, it remains unclear whether PM<sub>2.5</sub> alters DNA methylation and thereby aggravates the pathogenesis of PD by regulating expression of key genes such as *PINK1* and *DJ-1*. Study of potential gene expression changes can provide better understanding of the disease itself and may become a therapeutic target for treatment.

In this study, we evaluated the impact of PM<sub>2.5</sub> on expression and methylation of the key PD-related genes *PINK1* and *DJ-1*. We measured the impact of PM<sub>2.5</sub> on dopaminergic neurons in the substantia nigra (SN). In addition, we induced PD in rats by treating with rotenone and assessed aggravation of PD by PM<sub>2.5</sub> in these rats. Then, we measured expression and methylation of *PINK1* and *DJ-1* in SN after different times of exposure to PM<sub>2.5</sub>. Finally, we verified the animal results with SH-SY5Y cells and measured the effect of PM<sub>2.5</sub> on misregulation of DNA methylation of the *PINK1* and *DJ-1* genes.

## Results

### PM<sub>2.5</sub> concentration description

To observe the effects of PM<sub>2.5</sub> on animals over different time periods, we monitored atmospheric PM<sub>2.5</sub> concentrations at 3, 6 and 12 months and found that the average daily concentrations of PM<sub>2.5</sub>, which was 54.16 µg/m<sup>3</sup> during the first 3-month period, 52.58 µg/m<sup>3</sup> in the 6-month period, and 44.64 µg/m<sup>3</sup> in the 12-month period. Figure 1a shows the level of average concentration of PM<sub>2.5</sub> monitored using an individual particle monitor. All animals in the PM<sub>2.5</sub> group were exposed to PM<sub>2.5</sub> levels above China's national air quality standard (15 µg/m<sup>3</sup>) and the World Health Organization guideline (5 µg/m<sup>3</sup>).

### Effects of PM<sub>2.5</sub> on body weight

The animal weights were monitored monthly, and the results showed that the PM<sub>2.5</sub> group experienced a significant decrease in weight gain from Month 1 to Month 9 compared to the FA group (Fig. 1b). However, there was no significant difference in weight gain between the two groups from Month 10 to Month 12.

### PM<sub>2.5</sub> accelerated the loss of dopaminergic neurons in the substantia nigra of PD rat model

The average value of filtered air-exposed and vehicle-administered in each month was used as the control benchmark (100%). Compared with the filtered air-exposed, TH-positive cells were significantly decreased by 6.49% in the PM<sub>2.5</sub>-exposed; compared with the vehicle-administered, TH-positive cells were significantly decreased by 22.16% in the rotenone-administered at 3 months (Fig. 2a and b). Compared with the filtered air-exposed, TH-positive cells were significantly decreased by 5.23% in the PM<sub>2.5</sub>-exposed; compared with the vehicle-administered, TH-positive cells were significantly decreased by 52.99% in the rotenone-administered at 6 months (Fig. 2c and d). Compared with the filtered air-exposed, TH-positive cells were significantly decreased by 12.24% in the PM<sub>2.5</sub>-exposed; compared with the vehicle-administered, TH-positive cells were significantly decreased by 60.17% in the rotenone-administered at 12 months (Fig. 2e and f).

3 months: PM<sub>2.5</sub>-exposed (n = 12) vs filtered air-exposed (n = 12): F (1, 20) = 16.21, P = 0.0007; rotenone-administered (n = 12) vs vehicle-administered (n = 12): F (1, 20) = 189.1, P < 0.0001; interaction effect: F (1, 20) = 0.3146, P = 0.5811.

6 months: PM<sub>2.5</sub>-exposed (n = 12) vs filtered air-exposed (n = 12): F (1, 20) = 3.299, P = 0.0844; rotenone-administered (n = 12) vs vehicle-administered (n = 12): F (1, 20) = 338.1, P < 0.0001; interaction effect: F (1, 20) = 0.9893, P = 0.3318.

12 months: PM<sub>2.5</sub>-exposed (n = 12) vs filtered air-exposed (n = 12): F (1, 20) = 34.50, P < 0.0001; rotenone-administered (n = 12) vs vehicle-administered (n = 12): F (1, 20) = 833.9, P < 0.0001; interaction effect: F (1, 20) = 0.03124, P = 0.8615.

Significance of pairwise comparisons (n = 6): ns = non-significant; \*p < 0.05; \*\*p < 0.01; \*\*\*p < 0.001; \*\*\*\*p < 0.0001.

### PM<sub>2.5</sub> decreased the levels of *DJ-1* and *PINK1* mRNAs in PD rat model

To determine whether exposure to PM<sub>2.5</sub> affected the mRNA levels of *PINK1* and *DJ-1*, we measured *PINK1* and *DJ-1* mRNAs in the SN. Real-time RT-PCR results showed that 3 months of exposure induced a 60% reduction in *PINK1* compared with the FA group (Fig. 3a), whereas there was no difference in *DJ-1* mRNA level (Fig. 3b). However, when the exposure time was increased to 6 months, the reduction in *PINK1* mRNA level was nearly 75% (Fig. 3c), and a significantly greater reduction (nearly 50%) was also found in *DJ-1* (Fig. 3d). We observed still further reductions of mRNA levels of *PINK1* and *DJ-1* after 12 months of exposure (Fig. 3e and f).

### PM<sub>2.5</sub> resulted in hypermethylation of CpG islands in *PINK1* and *DJ-1* genes in PD rat model

By using the UCSC Genome Browser database, we found typical CpG islands around the promoters of the rat *PINK1* and *DJ-1* genes. There were 55 CG sites within the entire length of the CpG islands of both genes (Fig. 4a and e). Methylation status of the CpG islands was determined by bisulfite sequencing. Exposure to PM<sub>2.5</sub> for 6 months resulted in a 6.06% increase in methylation of the *PINK1* gene compared with 2.42% for the control (Fig. 4c). For the *DJ-1* gene, 6 months of exposure resulted in an increased methylation level from 2.4–7.27% (Fig. 4g). For 12 months exposure to PM<sub>2.5</sub>, the methylation level was further increased, reaching 9.30% and 12.73% in the *PINK1* and *DJ-1* genes, respectively (Fig. 4d and h); 3 months exposure to PM<sub>2.5</sub> had no effect on the methylation level on both genes (Fig. 4b and f).

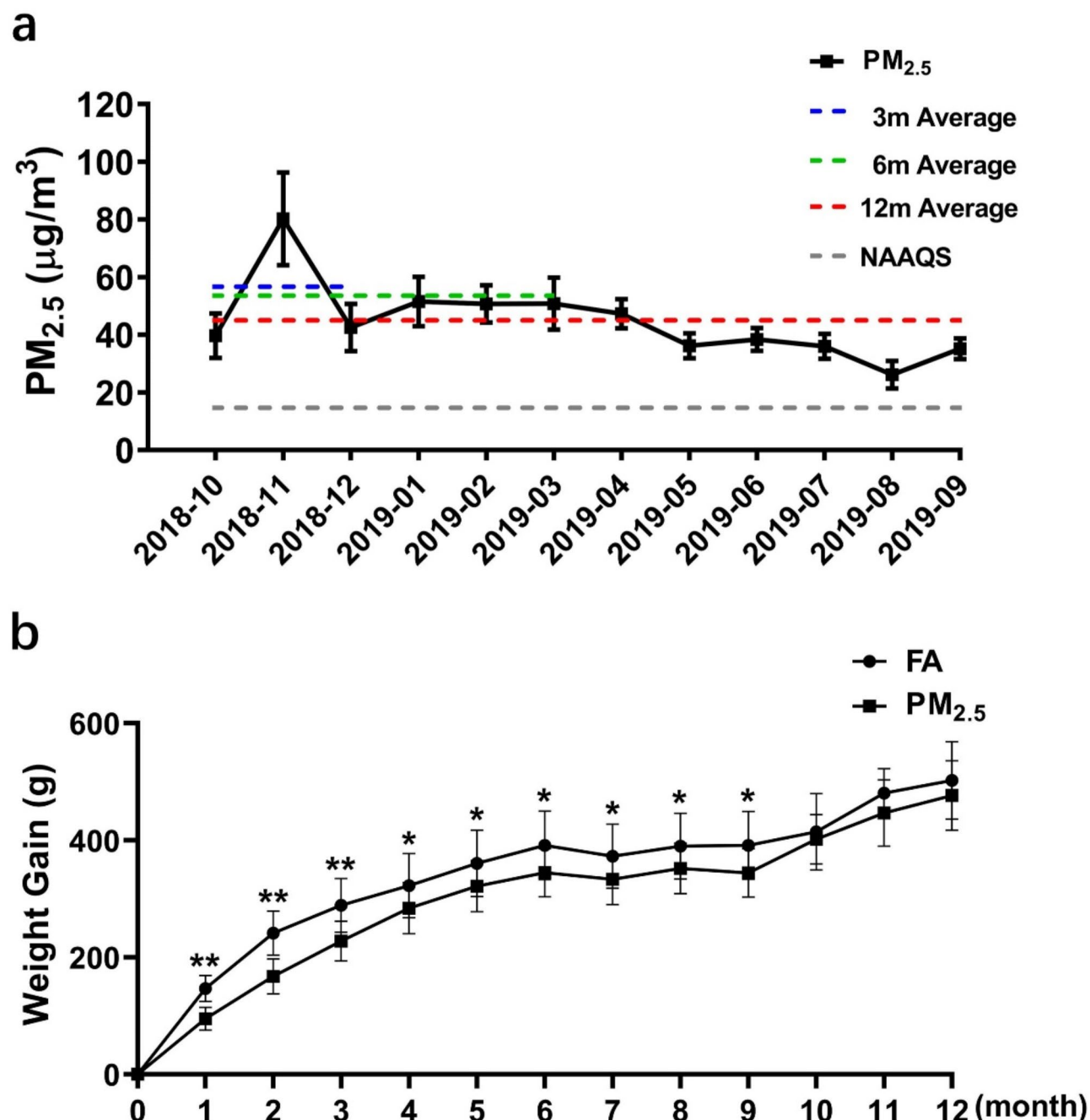


**Fig. 1.** The average concentration of PM<sub>2.5</sub> was higher than NAAQS and PM<sub>2.5</sub> resulted the lower body weight. **(a)** The level of average concentration of PM<sub>2.5</sub> monitored using an individual particle monitor. **(b)** Rat body weight gained every month in both groups (n = 20). \**p* < 0.05 compared to control, \*\**p* < 0.01 compared to control.

#### DEP resulted in decreased cell viability in PD cell model

We treated human neuroblastoma SH-SY5Y cells with DEP at 2.5, 5, 10, 20, 40, 80, 160, and 320 μg/ml for 24 h. The LD<sub>50</sub> (median lethal dose) was 40 μg/ml by viable cells counting (Fig. 5a) and LDH assay (Fig. 5b).

#### DEP repressed transcription of *PINK1* and *DJ-1* genes in PD cell model

In the forgoing animal study, we found that PM<sub>2.5</sub> resulted in a decrease in expression of the *PINK1* and *DJ-1* genes. To confirm this effect in vitro, we performed quantitative RT-PCR to measure the *PINK1* and *DJ-1* mRNA levels in SH-SY5Y cells. Under the condition of DEP concentration of 40 g/ml, the level of *PINK1* mRNA was significantly reduced at 6 h and 24 h (Fig. 6a), while the level of *DJ-1* mRNA was also significantly reduced at 24 h (Fig. 6b).

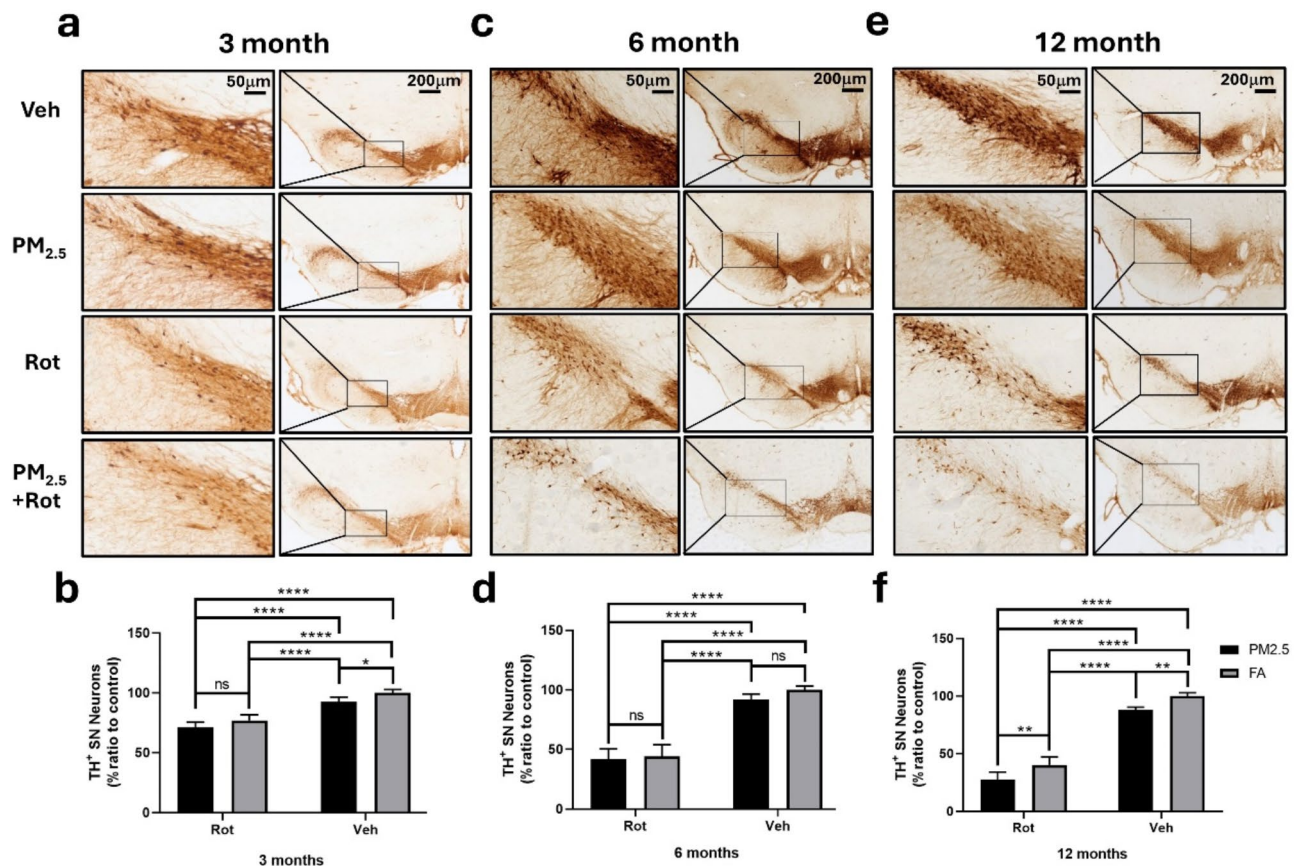


**Fig. 2.** PM<sub>2.5</sub> accelerated the loss of dopaminergic neurons in the SN. TH expression in SN sections was assessed by immune-histochemistry. (a, c, e) Immune-histochemistry staining results for 3, 6, and 12 m. (b, d, f) Quantitative analysis of TH-positive neurons. Statistical analysis was performed by two-way ANOVA.

### DEP resulted in hypermethylation of CpG islands in *PINK1* and *DJ-1* genes in PD cell model

Using the UCSC Genome Browser database, we identified 69 and 55 CG sites in the entire length of human *PINK1* and *DJ-1* CpG islands (Fig. 7a and c). Compared with the methylation level of the control group (2.42%), after 6 and 24 h of DEP treatment, the methylation level of the *PINK1* gene significantly increased to 6.28% and 11.59%, respectively (Fig. 7b). Likewise, in comparison with the methylation level of the control group (1.82%), the methylation level of the *DJ-1* gene significantly rose to 8.48% after 24 h of DEP treatment (Fig. 7d).

### Discussion

Epidemiological studies indicate that exposure to PM<sub>2.5</sub> is associated with an increased risk of developing Parkinson's disease and other neurological disorders<sup>6,17</sup>. Despite extensive research on the relationship between PM<sub>2.5</sub> and Parkinson's disease, the underlying molecular mechanisms remain largely unexplored. Therefore, our objective was to elucidate the mechanisms through which PM<sub>2.5</sub> exacerbates Parkinson's disease. In this study, we provide robust evidence that PM<sub>2.5</sub> can accelerate development of PD. The effect is based on the dysregulation of key PD-related genes, notably *PINK1* and *DJ-1*. Further, abnormal gene expression may be related to increased DNA methylation. First, we found that PM<sub>2.5</sub> caused the loss of dopaminergic neurons in the SN. The neurotoxin rotenone can damage dopaminergic neurons, and PM<sub>2.5</sub> can lead to further dopaminergic neurons loss induced by rotenone. Second, PM<sub>2.5</sub> decreased *PINK1* and *DJ-1* expression and increased methylation of the CpG islands of the *PINK1* and *DJ-1* genes. Third, treating SH-SY5Y cells with DEP produced similar effects as observed in animal experiment.

Our study shows that the weight of the PM<sub>2.5</sub> group significantly decreased during the first to ninth month, which is consistent with previous research findings. In an animal experiment using C57BL/6 J mice as in vivo models, the researchers administered PM<sub>2.5</sub> (2.5 mg/kg, inhalation) and rotenone (30 mg/kg, intraperitoneal injection) to the mice for 28 days<sup>9</sup>. The study found that the weight of the rotenone group mice was significantly lower than that of the control group from 4 to 28 days. Furthermore, there was a significant difference between the rotenone group and the PM<sub>2.5</sub> + rotenone group, indicating that PM<sub>2.5</sub> affects the body weight of PD mice. Although the observation period was only 28 days, the result is consistent with our findings. The potential mechanism by which PM<sub>2.5</sub> affects body weight may involve metabolic disorders caused by air pollution, which are closely related to body weight<sup>18</sup>. However, in epidemiological studies, the impact of air pollution on weight

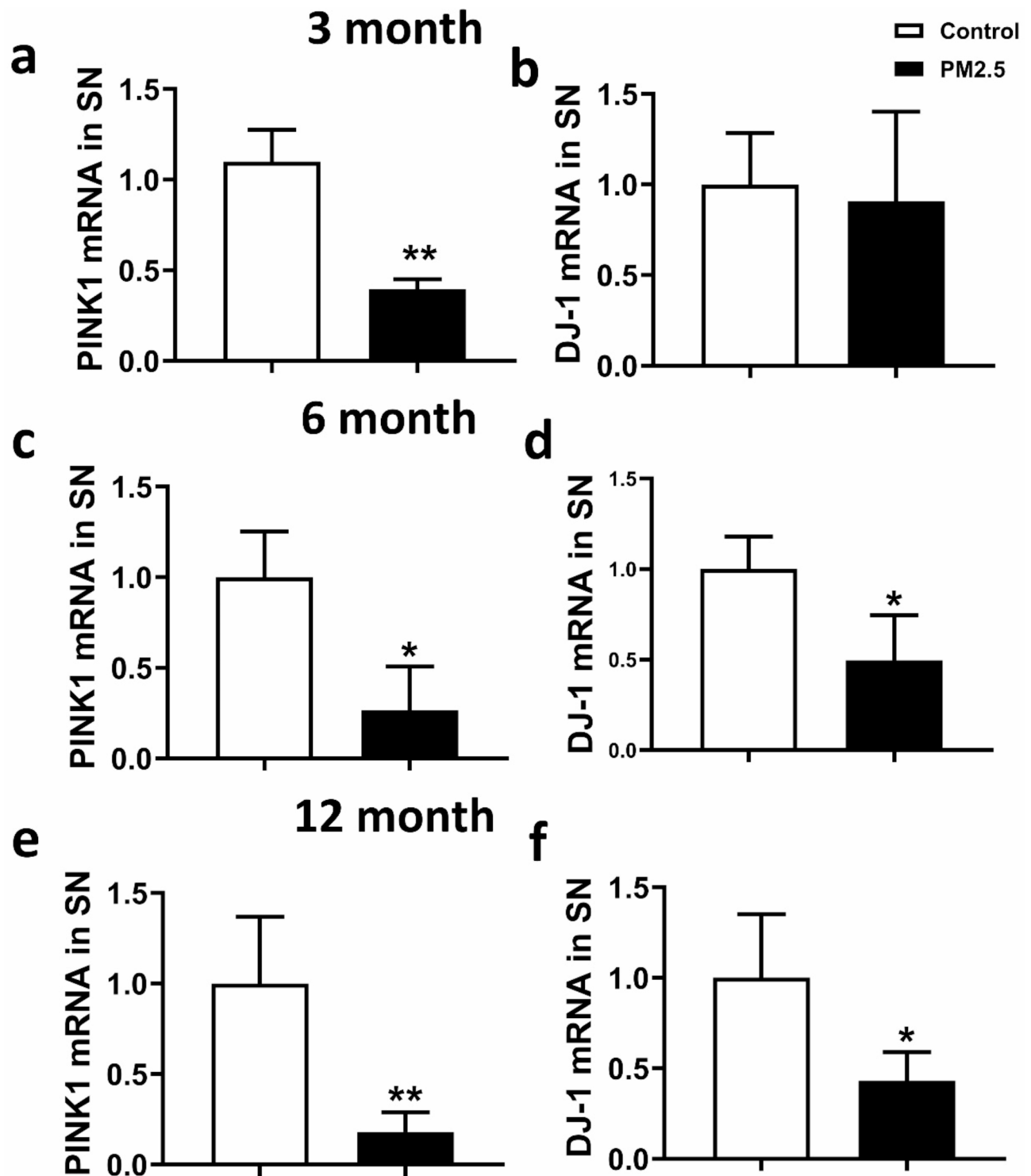


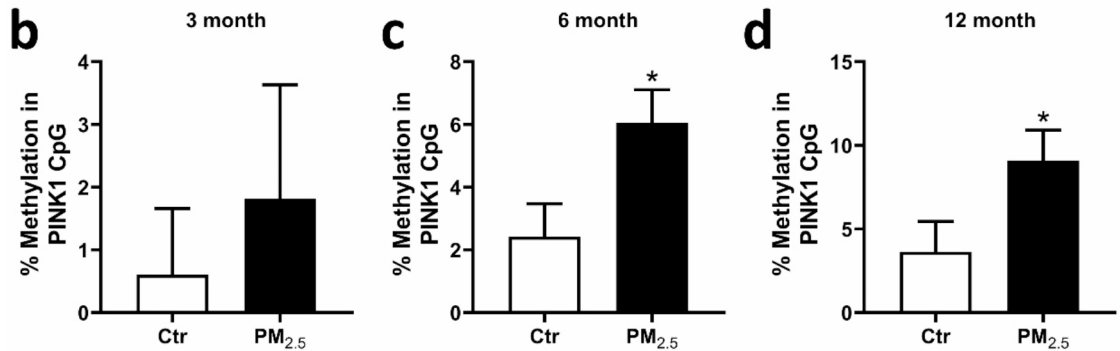
**Fig. 3.** PM<sub>2.5</sub> down-regulated the transcription of *PINK1* and *DJ-1* genes in rats' model. The mRNA levels of both genes were assessed by real-time RT-PCR. (a, c, e) The transcription level of *PINK1* gene at 3, 6 and 12 m in control and PM<sub>2.5</sub> groups. (b, d, f) The transcription level of *DJ-1* gene at 3, 6, and 12 m in both groups. Statistical analysis was performed by ANOVA. Significance (n=8): \**p* < 0.05 compared to control, \*\**p* < 0.01 compared to control, \*\*\**p* < 0.001 compared to control.

remains highly controversial and may vary depending on factors such as gender, age group, and type of air pollutant<sup>19–21</sup>. Therefore, further in-depth research is needed to clarify this issue.

Previous studies have indicated that PM<sub>2.5</sub> can trigger neuroinflammation, leading to the loss of dopaminergic neurons and the formation of Lewy bodies, while inducing mitochondrial dysfunction to stimulate the

**a** 5'--3' CpG island of *PINK1* (55CG sites)

CGgcCGcaaggccctgCGtCGcctCGggccCGtaccaCGaactgcCGttggattCGCGcCGccag  
 cccagccacCGactggCGgaagaagCGgtagCGgtcCGggagggggagccCGagCGgaCGCGgc  
 tgtgtccCGggcttgagaccCGgcCGgaCGctctcCGCGccccagggccCGcacCGgggcCGgg  
 ctgccccagccgtgagacCGggccCGgcttgggagCGaagCGcagcagcagCGccCGacccagctg  
 caggcctCGgcccagtgctgtCGcacCGccatggtggCGCGGCGacCGgagccagctgccacCGc  
 caaaaCGtcCGaaaagctgaggacaacaacaacttCGggggCGgtgcctatgCGcaagCGcagg  
 gggCGgtcccCGgcagttctctgcacagcaCGtgggggCGcaaccCGctcttctcCGcatcCG

**e** 5'--3' CpG island of *DJ-1* (55CG sites)

CGCGaaCGagagcagtttagcCGccactgtgaagcaCGttcCGCGtggttttctcCGCGgttcccag  
 gcatcaaaaactttggttaagccttccagtaactgtgctCGccacaaccCGgaggggggctgtgcagagctct  
 agccCGgcatgcacCGCGgcCGcCGccccagccCGcCGggccCGgatcctcccCGggcaaCGg  
 gCGgaccacagccCGgcctcctcctgcccCGgggCGctgacctgcagcCGCGcctcctccacccaCG  
 CGaagccacagacagtccCGcaggaacacCGtaccCGgctcagtCGcacagattgtacacaacaCG  
 catgCGcactatgCGCGatgaggctgCGcaccctcttcttCGcctCGgtgtgCGtcaCGtcCGgtt  
 gagctcaggaccCGggatgatgagtgaacagaggatactaCGCGgcCGtttttttttttttggccCGaa  
 gttggggacCGaagCGctctaccactgagttaaatccccaaccctgCGCGgcCGttttaacaCGccctt  
 ccctccccaaccaactgtactgagcacctgCGagCGcctgCGCGgttga

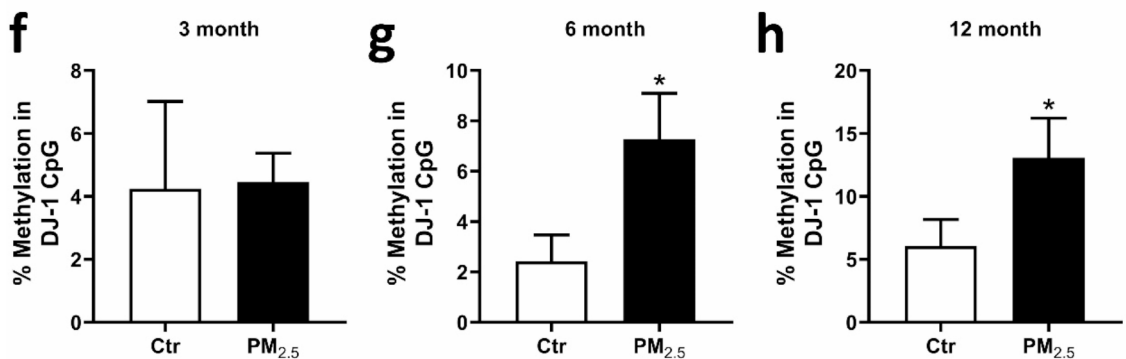


**Fig. 4.** The CpG islands and 5' up-streamed region around *PINK1* and *DJ-1* promoters in rats. Methylation status of the CpG islands was analyzed using Bisulfite sequencing. (**a**, **e**) 55 CpG sites in the CpG islands of *PINK1* and *DJ-1*, respectively. (**b**, **c**, **d**) Methylation level of *PINK1* CpG islands at 3, 6, and 12 m in both control and PM<sub>2.5</sub> groups. (**f**, **g**, **h**) Methylation level of *DJ-1* CpG islands. Significance (n = 5): \* $p < 0.05$  compared to control, \*\* $p < 0.01$  compared to control.

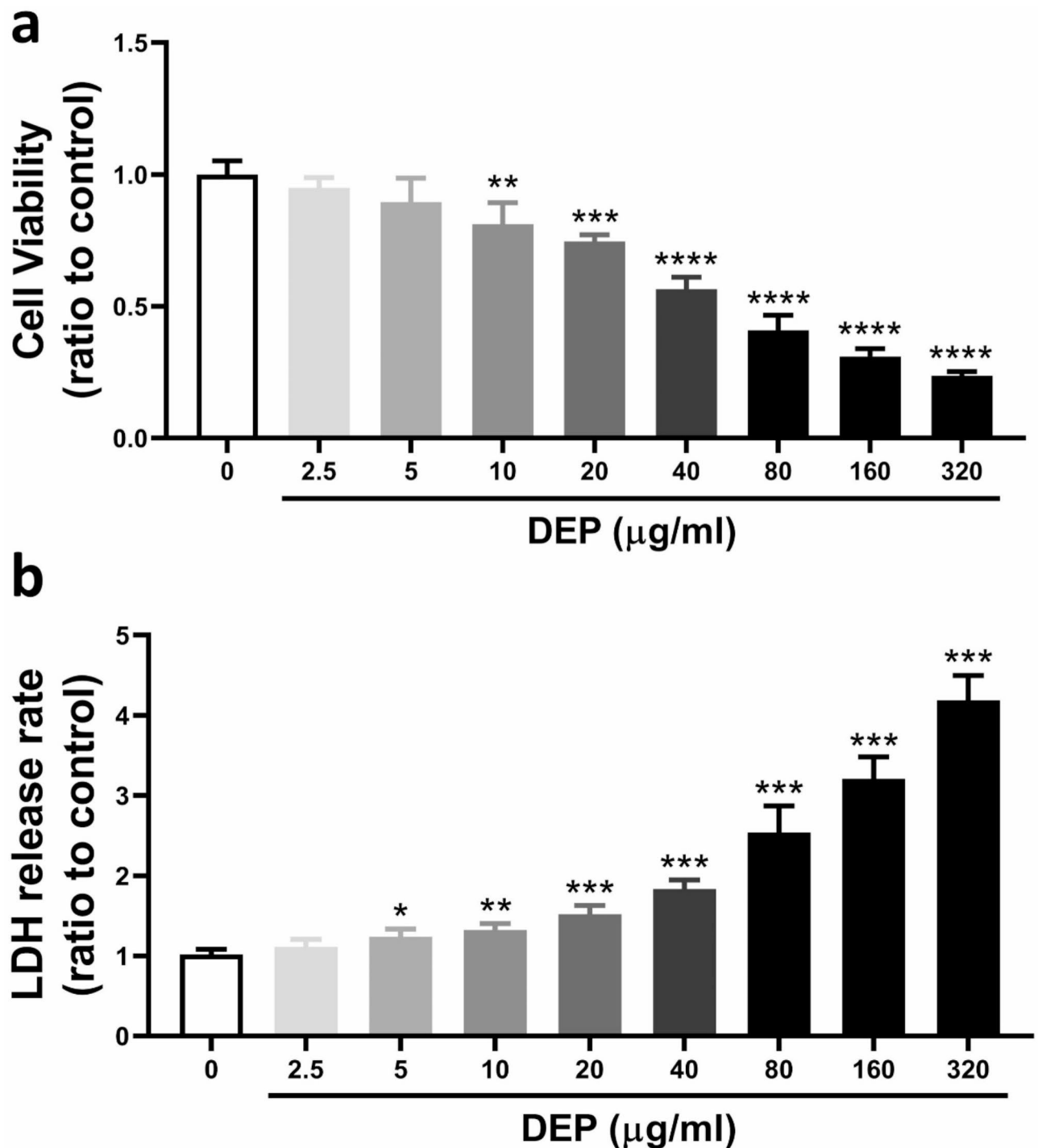


**Fig. 5.** DEP reduced cell viability. Optimal  $\text{PM}_{2.5}$  treated concentration was determined in SH-SY5Y cells by evaluating cell viability and cytotoxicity with viable cells counting and LDH assays, respectively. **(a, b)** Cell viability and cytotoxicity were detected in SH-SY5Y cells with viable cells counting **(a)** and LDH **(b)** assays. Significance ( $n=3$ ): \* $p < 0.05$  compared to control, \*\* $p < 0.01$  compared to control, \*\*\* $p < 0.001$  compared to control. DEP: Diesel exhaust  $\text{PM}_{2.5}$ .

production of reactive oxygen species (ROS), thereby aggravating neuronal damage<sup>9,22–24</sup>. In this study, we found that, similar to neurotoxin rotenone,  $\text{PM}_{2.5}$  causes the loss of dopaminergic neurons in the SN, and  $\text{PM}_{2.5}$  can further exacerbate the loss of dopaminergic neurons caused by rotenone. In addition, similar studies have observed that short-term  $\text{PM}_{2.5}$  exposure can worsen animal behavior<sup>9</sup>, but this aspect was not tested in our study. Therefore, the behavioral changes caused by long-term exposure to  $\text{PM}_{2.5}$  still need further investigation.

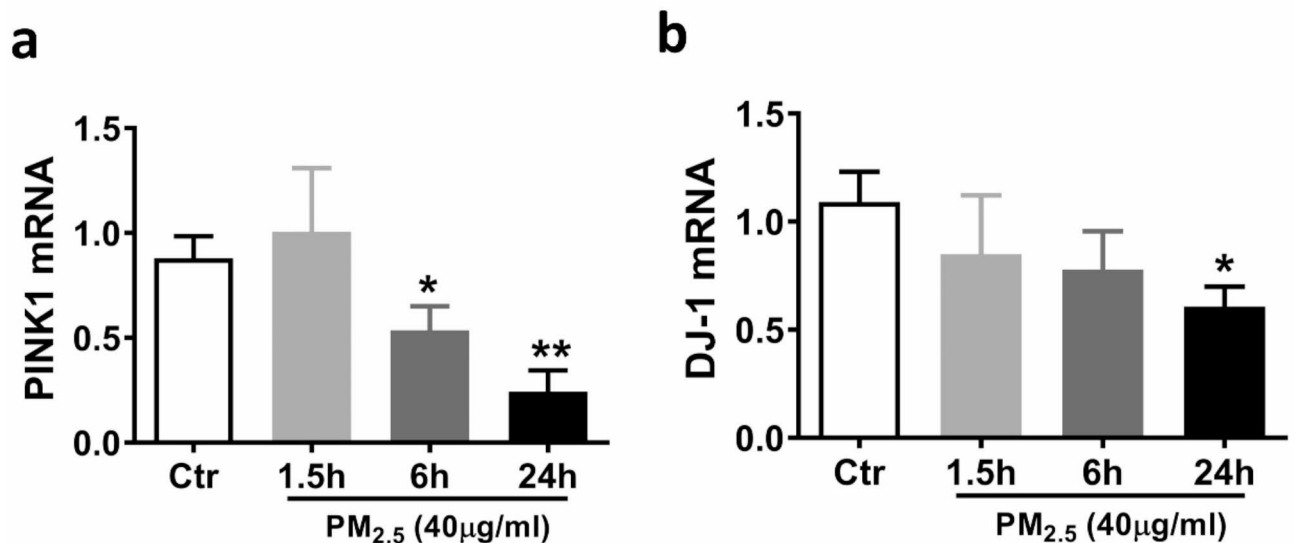
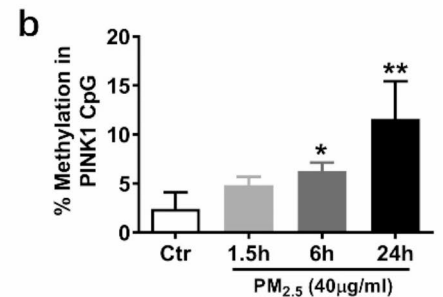


**Fig. 6.** DEP down-regulated the transcription of *PINK1* and *DJ-1* genes in SH-SY5Y cells. SH-SY5Y cells were treated with 40 µg/ml of PM<sub>2.5</sub> for 1.5, 6, and 24 h. The mRNA levels of *PINK1*(a) and *DJ-1*(b) were assessed by real-time RT-PCR. Statistical analysis was performed by ANOVA. Significance (n = 3): \**p* < 0.05 compared to control, \*\**p* < 0.01 compared to control, \*\*\**p* < 0.001 compared to control. DEP: Diesel exhaust PM<sub>2.5</sub>.

**a** 5'–3' CpG island of *PINK1* (69CpG sites)

accagcatagCGccccCGCGcCGagtCGgggaactgcCGCGggggcCGggccCGcccc  
ccagcgctgCGcctgCGcagaggcacCGcccaagtgtgtgacCGgCGggggaCGcCG  
gtggtggCGgcagCGgCGctgCGggggcacCGggcCGCGgCGccaccatggCGgcgC  
GacaggCGctgggcCGCGcctgcagctgggtCGagCGctgctgctgCGttcaCGggcaag  
ccCGgcCGggcctaCGgctggggCGgcCGggccCGgCGgCGggctgtgCGCGggga  
gCGtccaggctgggcCGcaggacCGgCGCGgagcctCGcagggtCGggctCGggctccct  
aacCGtctcCGcttctcCGccagtCGgtggcCGggctggCGgCGCGgttcagCGgcagttC  
GtggtgCGggcctggggctgCGCGggccctgCGgcCGggcagctttctgacctCGggctag  
ggctgggacctcatCGaggaa



**c** 5'–3' CpG island of *DJ-1* (55 CpG sites)

tcccCGgtgccccCGcctcagtcCGagtagactCGgcCGgaCGtgaCGcagCGtgaggc  
caaggCGgCGtgagctgCGcagtggtgggctgagggaggcCGgaCGgCGCGCGtgCGt  
gtctggCGtgCGttcatttcagctggtgtggggtgagtggtaccacCGggcCGgggCGcCGC  
GtcCGcaggaagaggCGCGgggtgcaggtcagCGccagCGggggCGCGgCGcatgtgtg  
ggcCGtggtCGctgggCGgCGtgggggtgctggaCGgtgtccctgtgctggaCGgtgtccCGc  
tggtcagaacCGgCGCGgggctgggtCGgggcCGccctCGcttcCGgctccagtcCGgg  
ccctgtCGctggCGgttgatttgactgacCGccagCGtggtggcaaCGctgaagCGtcagaatc  
tctgcctaacctctCGcCGg

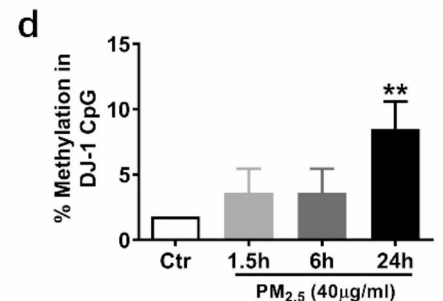


**Fig. 7.** The CpG islands and 5' up-streamed region around *PINK1* and *DJ-1* promoters in human cells. Methylation status of the CpG islands was analyzed using Bisulfite sequencing. (a, c) 69 and 55 CpG sites in the CpG islands of *PINK1* and *DJ-1*, respectively. (b, d) Methylation level of *PINK1* and *DJ-1* CpG islands at 1.5, 6 and 24 h treated DEP. Significance (n = 3): \**p* < 0.05 compared to control, \*\**p* < 0.01 compared to control. DEP: Diesel exhaust PM<sub>2.5</sub>.

Our study found that exposure to PM<sub>2.5</sub> also leads to the loss of dopaminergic neurons, as well as downregulation of *PINK1* and *DJ-1* mRNA expression. Previous studies have found that the loss of dopaminergic neurons is correlated with low expression of *PINK1*. In previous studies on animals, cells, and organoids, *PINK1* deficiency impairs adult neurogenesis of dopaminergic neurons<sup>25–27</sup>. In a robust vertebrate model of *PINK1* deficiency, the *PINK1*<sup>-/-</sup> zebrafish, Th1 + neurons of the TPp and PVO are found in comparable numbers to those in young adult wild-type fish, but thereafter showed a significant decline<sup>25</sup>. Similarly, impaired dopaminergic neurogenesis was observed in human tissue organoid models with *PINK1* deficiency<sup>25</sup>. *PINK1* and *NOTCH* interact non-

classically in mitochondria, and *PINK1* deficiency significantly inhibits the proliferation of human neural stem cells (NSCs)<sup>26</sup>. Growth inhibition was also observed in mouse *PINK1* knockout NSCs, which was associated with mitochondrial dysfunction<sup>32</sup>. For *DJ-1*, previous studies have shown that reducing *DJ-1* expression can affect the function of dopaminergic neurons, and the dopaminergic neurons in the substantia nigra of *DJ-1* mutant mice are functionally impaired<sup>28,29</sup>. *DJ-1* protein has characteristics such as molecular chaperone, protease, glutathione peroxidase, transcriptional regulator, and *DJ-1* protein prevents neurodegenerative diseases by regulating oxidative stress and mitochondrial function, as well as its role in transcription and signal transduction<sup>30–32</sup>. Based on the above studies, we can conclude that the downregulation of *PINK1* mRNA expression leads to a decrease in the number of dopaminergic neurons, while the downregulation of *DJ-1* mRNA expression affects the function of dopaminergic neurons. Therefore, we hypothesize that the loss of dopaminergic neurons observed in our study, which was caused by exposure to PM<sub>2.5</sub>, may be due to the downregulation of *PINK1* mRNA expression. In addition, PM<sub>2.5</sub>-induced *DJ-1* mRNA is likely to exert an influence on the function of dopaminergic neurons. Previously studies have proven that DNA methylation has been shown to be pivotal to the occurrence and development of PD<sup>33,34</sup>, including the regulatory role of PD-related genes such as *α-synuclein*, *Parkin*, *PINK1*, *DJ-1*. Yang's study showed that CpG demethylation was induced by MPP<sup>+</sup> mediated up-regulation of *SNCA* transcription in neurotoxin-induced PD<sup>35</sup>. Tarale et al. performed chronic manganese exposure of human SH-SY5Y cells and found that integration of DNA methylation data with gene expression revealed epigenetic alterations to *PINK1* and *Parkin* genes that were critical for the onset of Parkinsonism<sup>36</sup>. Both short and long-term exposure to ambient air pollution resulted in global changes to DNA methylation<sup>37,38</sup>. In our study, we found that rats which received more than 6 months of PM<sub>2.5</sub> exposure had elevated DNA methylation of CpG islands of the *PINK1* and *DJ-1* genes, and cells-based data showed that long-term (6 or 24 h) treated with DEP resulted in increased DNA methylation of CpG islands. Thus, our results confirmed that long-term exposure to PM<sub>2.5</sub> can lead to changes in DNA methylation for some genes. Further, the decreased gene expression associated with the aforesaid treatments can be explained by increased DNA methylation.

Our study had several limitations. First, in the cell-based experiment, we did not test an inhibitor of DNA methylation such as 5-Aza to determine whether DNA methylation changes could be reversed. Second, other investigators have found that neurotoxins can induce misregulation of DNA methylation<sup>35</sup>. However, we did not determine whether rotenone itself affected DNA methylation. Third, although much evidence confirms that DNA methylation has a key function in the occurrence and development of PD, studies on specific regulatory mechanisms are still limited. For example, we did not determine which DNA methyltransferase(s) was responsible for the increased methylation of the *PINK1* and *DJ-1* genes or which signaling pathways were involved in the process.

In summary, our study revealed that exposure to PM<sub>2.5</sub> leads to the loss of dopaminergic neurons in the substantia nigra, aggravates the development of PD by inducing dysregulation of DNA methylation, resulting in decreased expression of the PD-related genes *PINK1* and *DJ-1*.

## Methods

### PD rat model

The animal protocols in this study were approved by the Ethics Committee for Animal Experimentation at Capital Medical University (Beijing, China), and all experimental procedures were performed in accordance with the National Institute of Health Guide for the Care and Use of Laboratory Animals. 4-week-old male Sprague–Dawley rats were purchased from Vital River Laboratory Animal Technology Co., Ltd. (Beijing, China) and randomly distributed into PM<sub>2.5</sub>-exposed (n = 72) or filtered air (FA) groups (n = 72). Each group was subdivided into a rotenone-administered group (2 mg/kg) for 4 w (n = 36) or a vehicle-administered group (n = 36). The rats were housed in a controlled room at a temperature of 24 °C with a standard 12-h light/dark cycle and had free access to food and water. The rats were housed for 3 months, 6 months, and 12 months, respectively. The diagram of the experimental design is in Fig. 8.

### Rotenone administration

The rotenone was dissolved in DMOS and diluted in sterile sunflower oil (2% final DMSO concentration and 98% final sunflower oil concentration)<sup>39</sup>. The rotenone-administered group received supplementation of rotenone (2 mg/kg/d) for 30 days before tissue extraction respectively at 3, 6 and 12 months. The rotenone solution was given by intragastric administration. The final working concentration of rotenone is re-prepared every two days and stored in a light-protected ambient temperature environment.

### Exposure to PM<sub>2.5</sub>

Animals were exposed to PM<sub>2.5</sub> or FA for 24/7 for 3 months (from October 11, 2018 to January 10, 2019), 6 months (from October 11, 2018 to April 10, 2019), and 12 months (from October 11, 2018 to October 10, 2019) using our real-world PM<sub>2.5</sub> exposure system described previously<sup>40</sup>. The mean daily PM<sub>2.5</sub> concentration in each chamber was monitored by an individual portable fine particulate monitor. PM<sub>2.5</sub> was monitored using a portable fine particulate monitor (pDR1500, Thermo Fisher Scientific Inc., USA) at Peking Union Medical College Hospital (located at 116°22'05"E, 39°54'50"N) in Beijing, China. The condition of FA rats in the experiment was the same as that of PM<sub>2.5</sub> rats in all aspects; the difference was that the improvement of air quality caused by the placement of a high-efficiency particulate air filter in the intake valve position leads to the removal of all PM<sub>2.5</sub> from the FA flow. The annual average PM<sub>2.5</sub> National Ambient Air Quality Standard (NAAQS) in China was recorded.

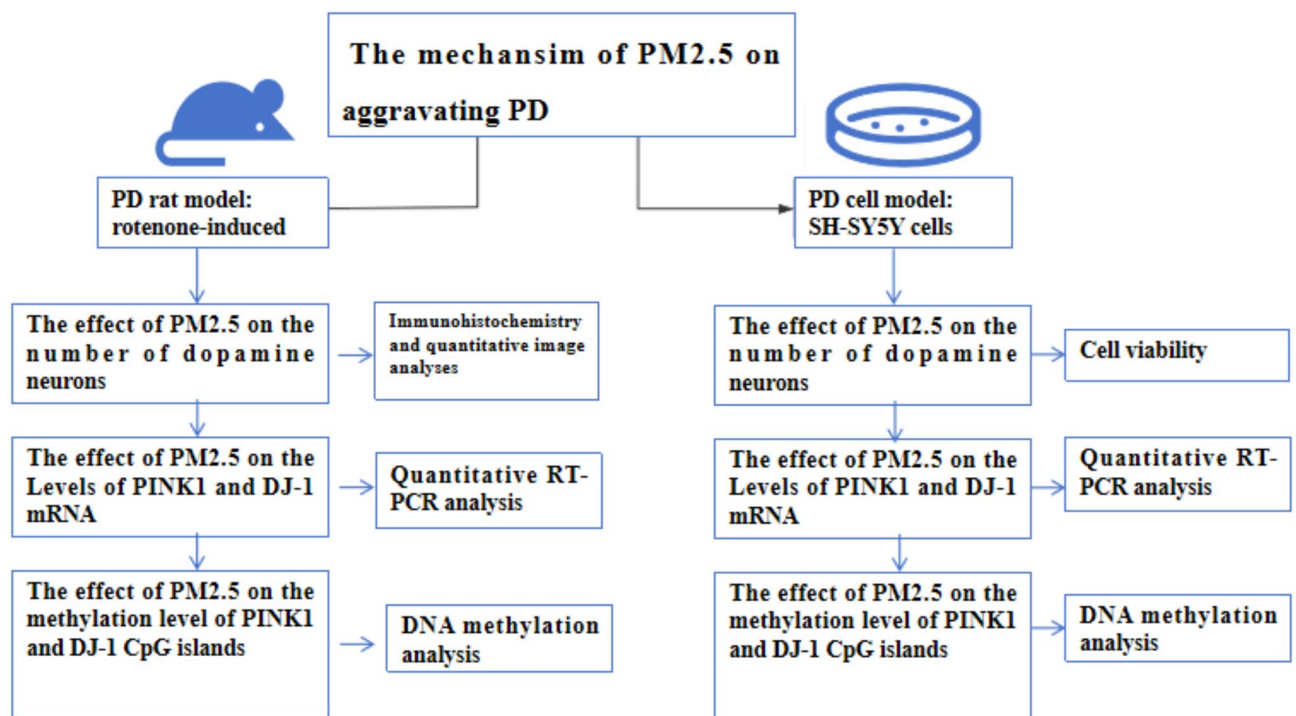


**Fig. 8.** The diagram of the experimental design.

### Immunohistochemistry and quantitative image analyses

At the end of the treatment animals ( $n=6/\text{group}$ ) were sacrificed under general anesthesia induced by a combination of ketamine hydrochloride (80 mg/kg) and xylazine hydrochloride (4 g/kg) through intraperitoneal administration and transcardially perfused with 0.9% sodium saline (room temperature), followed by 4% paraformaldehyde (PFA)/phosphate-buffered saline (PBS) (pH 7.4, ice-cold). Brains were post fixed for 12 h in 4% PFA and dehydrated in 20% and 30% sucrose in PBS, respectively. Brains were frozen and sectioned coronally (30  $\mu\text{m}$ ) and placed into a tissue collection solution (50% 0.01 M PBS/50% glycerol) and stored at  $-20^\circ\text{C}$ . The sections were permeabilized in PBS containing 0.3% Triton X-100, blocked in 5% normal horse serum, and then incubated overnight at  $4^\circ\text{C}$  with an anti-TH antibody (1:2000, Sigma). After washing three times with PBS, sections were respectively incubated with a biotinylated second antibody (1:200; Zhongshan Golden Bridge Biotechnology Co., Beijing, China) and an AB work solution (1:1:100) for 30 min at  $37^\circ\text{C}$  (Vector Laboratories, USA). DAB solutions (a drop of DAB to 2 ml substrate liquid) were used to visualize the antibody. Sections were fixed on slides and cover slipped with a water-soluble mounting medium. The sections were imaged with a bright-field microscope. The estimated number of TH+ cells was calculated based on the neuronal count and the corresponding sampling probabilities. The quantity of TH immunoreactive cell bodies in the SN was quantified using Stereo Investigator software, Version 2017.02.2 (09/27/2017) (MBF Bioscience, USA)<sup>39,41,42</sup>. The average number of SN sections was six in a 1:6 series. The number of TH cell bodies in each counting frame was determined by focusing each part with a 20-times objective lens. The total count of TH cell bodies in each section was computed by the software. A coefficient of error below 0.10 was deemed acceptable. Quantitative results for TH cell bodies were expressed as a percentage relative to the control side. Blind statistical analysis utilizing stereology methods was conducted for each experiment.

### Cell culture and DEP treatment

SH-SY5Y neuroblastoma cells were cultured in Dulbecco's modified Eagle's medium (DMEM, Hyclone, Logan, UT, USA) supplemented with 10% FBS (Cat# SV30087.02, Hyclone, Logan, UT, USA), 100 IU/ml penicillin, and 100  $\mu\text{g}/\text{ml}$  streptomycin (Gibco, Grand Island, NY, USA) in a 5%  $\text{CO}_2$  humidified atmosphere at  $37^\circ\text{C}$ . The medium was routinely changed every 2 days, and cells were passaged every 4 days. Diesel exhaust  $\text{PM}_{2.5}$  (DEP, a source of fine particle pollution that contains a high proportion of ultrafine particles) was obtained from the National Institute of Standards and Technology (SRM 2975, NIST, Gaithersburg, MD, USA). According to the analysis certificate of the standard reference material 2975, the average particle size distribution of DEP2975 was approximately 1.62  $\mu\text{m}$ . DEP was suspended in the DMEM cell culture medium. To minimize aggregation to the greatest extent, the particle suspension was subjected to sonication for 15 min and rotation before dilution and administration.

### Cell viability

Viable cells counting: Cells were harvested and stained with 0.04% Trypan blue (Life Technologies, Inc., Gaithersburg, MD, USA). Viable cells were counted under a microscope using a blood cell counter. And the cell

Gene	Gene Bank ID	Sequences 5'–3'
Rat-PINK1	NM_001106694.1	Forward: GGACCGCTACCGTTCTTC
		Reverse: CTCCTCGATCAGCCCCAAC
Rat-DJ-1	NM_001277249.1	Forward: GGTGTCGAGCGTTCGTAGC
		Reverse: CATGGAGGGCTTGCTGTAATATC
Rat-GAPDH	NM_017008.4	Forward: GGTGTCGAGCGTTCGTAGC
		Reverse: CATGGAGGGCTTGCTGTAATATC
Huam-PINK1	NM_032409.3	Forward: CTCCTTAACCGTCTCCGTTCT
		Reverse: GGCCCCGGCTTGCTTTT
Huam-DJ-1	NM_001123377.1	Forward: CTCCTTAACCGTCTCCGTTCT
		Reverse: GGCCCCGGCTTGCTTTT
Human-GAPDH	NM_001256799.3	Forward: CTCCTTAACCGTCTCCGTTCT
		Reverse: GGCCCCGGCTTGCTTTT

**Table 1.** Primers used in RT-PCR.

Gene	
Rat-PINK1-BSP-F1	TAAGGATGATTTTGGTTGCGTTTT
Rat-PINK1-BSP-R1	CCTAACTCAACTTCTCATCTTAACCAAA
Rat-PINK1-BSP-F2	TAGTTCGAAGGTTAGGAAGATTGTT
Rat-PINK1-BSP-R2	TCAAAATACAACTAATAACCCAA
Rat-DJ-1-BSP-F1	TAGGTTGGGGGAGATTAATGGTGTT
Rat-DJ-1-BSP-R1	TAATTCAAACCTAATCCCAATCTAA
Rat-DJ-1-BSP-F2	TTAATTTTGTAGACGGTTTGTAT
Rat-DJ-1-BSP-R2	CGTAACCACTATCCTCTTAACCTTT

**Table 2.** Primers used in BSP methylation assay in rat study.

viability (%) was determined as the number of living cells/total number of cells (viable + non-viable cells)  $\times$  100. The experiment was carried out in triplicate.

Lactate dehydrogenase (LDH) assays: The LDH assay was carried out using a cytotoxicity detection kit (Roche Diagnostics, Mannheim, Germany) according to the manufacturer's instructions. LDH release was measured in a 100  $\mu$ l aliquot of supernatant, with 100  $\mu$ l preservation solution used as a blank to correct the optical density reading at 490 nm. The experiment was carried out in triplicate.

### Quantitative RT-PCR analysis

To measure *PINK1* and *DJ-1* mRNA expression, total RNA was extracted from the SH-SY5Y cells and tissues using TRIzol reagent (Cat# 15596-026, Life Technologies, California, USA) according to the manufacturer's instructions. The purified RNA was then reverse-transcribed into cDNA using the PrimeScript™ RT reagent Kit with gDNA Eraser (RR047B, TaKaRa). PCR primers were designed and synthesized by Invitrogen Company; the sequences are shown in Table 1. Quantitative RT-PCR analysis of the mRNA levels of *PINK1* and *DJ-1* was performed using the SYBR®Premix Ex Taq™ II (TliRNaseH Plus), ROX plus, (RR82LR, TaKaRa). GAPDH was chosen as the housekeeping gene. The real-time PCR program steps were: 95 °C for 5 min, 45 cycles at 95 °C for 5 s, 60 °C for 5 s, and 72 °C for 10 s, followed by 72 °C for 1 min.

### DNA methylation analysis

Predication of the *PINK1* and *DJ-1* CpG islands was performed using the UCSC Genome Browser database (<http://genome.ucsc.edu/>). Briefly, genomic DNA was extracted using a QIAamp DNA mini kit (Cat# 51304, QIAGEN, Hilden, Germany) according to the manufacturer's instructions. The integrity and purity of DNA were spectrophotometrically examined according to its A260/A280 absorption. A total of 50 ng of genomic DNA from each sample was bisulfite-treated with the Methylamp DNA Modification Kit (Epigentek, Farmingdale, NY, USA). To assay methylation status, the CpG islands of *PINK1* and *DJ-1* were divided into three segments amplified by PCR. PCR primers were designed and synthesized by Invitrogen Company; the sequences are shown in Tables 2, 3. The quality of bisulfite conversion was evaluated using the PCR products without methyl groups as the control. The methylation status was assayed by the Sequenom Mass ARRAY platform (JIA MEI Biolab, Beijing, China). Design methylated and unmethylated primers using Meth Primer software for PCR amplification of sequence differences before and after modification. The methylation ratios were generated by EpiTyper software version 1.0 (Sequenom, San Diego, CA, USA). The generated data were put into the EPI 3.1 Database (EpiData Association, Odense, Denmark) and analyzed with SPSS 11.5 software (McGraw-Hill Inc, New York, NY). Methylation frequency = Number of methylation of all clones measured in each sample/total CpG of that sample<sup>35,43</sup>.

Gene	
Cell-PINK1-BSP-F1	TGATGTTTATATTTAGGATTGTTTGA
Cell-PINK1-BSP-R1	CTCACCTAAATCTCCTAACAACACC
Cell-PINK1-BSP-F2	GAAAGTTATTGTTAGAGGCGTTAGT
Cell-PINK1-BSP-R2	CGCCGACTCTCCGCCTATTT
Cell-DJ-1-BSP-F1	GGTTCGGGAGGTTTGGATTAGAGTT
Cell-DJ-1-BSP-R1	CTCACTACCAACGACAACAACCTCAA
Cell-DJ-1-BSP-F2	GTTTATTATTAGGGTTGTTAGTTAGAA
Cell-DJ-1-BSP-R2	TAATAAACGACTAACCAATCCATA

**Table 3.** Primers used in BSP methylation assay in cell study.

### Statistical analyses

Statistical analysis was performed using Prism10 (GraphPad software, Inc., La Jolla, USA). Values were represented as means  $\pm$  SEM. Data were analyzed using one-way ANOVA followed by a Tukey's multiple paired comparison test as a post hoc test. A  $p$  value of  $<0.05$  was considered as statistically significant.

### Data availability

The authors agree to share any data on request. Any data from this study are available by contacting the corresponding author.

Received: 26 June 2024; Accepted: 5 February 2025

Published online: 28 March 2025

### References

- Qi, S. et al. Prevalence of Parkinson's disease: A community-based study in China. *Mov. Disord.* **36**, 2940–2944. <https://doi.org/10.1002/mds.28762> (2021).
- Russ, T. C., Reis, S. & van Tongeren, M. Air pollution and brain health: Defining the research agenda. *Curr. Opin. Psychiatry* **32**, 97–104. <https://doi.org/10.1097/YCO.0000000000000480> (2019).
- Li, B. et al. PM<sub>2.5</sub> exposure stimulates COX-2-mediated excitatory synaptic transmission via ROS-NF-kappaB pathway. *Chemosphere* **190**, 124–134. <https://doi.org/10.1016/j.chemosphere.2017.09.098> (2018).
- Calderon-Garciduenas, L. et al. Cerebrospinal fluid biomarkers in highly exposed PM<sub>2.5</sub> urbanites: The risk of Alzheimer's and Parkinson's diseases in young Mexico city residents. *Journal of Alzheimers Disease JAD* **54**, 597–613. <https://doi.org/10.3233/JAD-160472> (2016).
- Kasdagli, M. I., Katsouyanni, K., Dimakopoulou, K. & Samoli, E. Air pollution and Parkinson's disease: A systematic review and meta-analysis up to 2018. *Int. J. Hyg. Environ. Health* **222**, 402–409. <https://doi.org/10.1016/j.ijheh.2018.12.006> (2019).
- Fu, P., Guo, X., Cheung, F. M. H. & Yung, K. K. L. The association between PM<sub>2.5</sub> exposure and neurological disorders: A systematic review and meta-analysis. *Sci. Total Environ.* **655**, 1240–1248. <https://doi.org/10.1016/j.scitotenv.2018.11.218> (2019).
- Palacios, N. Air pollution and Parkinson's disease—evidence and future directions. *Rev. Environ. Health* **32**, 303–313. <https://doi.org/10.1515/reveh-2017-0009> (2017).
- Kirrane, E. F. et al. Associations of ozone and PM<sub>2.5</sub> concentrations with Parkinson's disease among participants in the agricultural health study. *J. Occup. Environ. Med.* **57**, 509–517. <https://doi.org/10.1097/JOM.0000000000000451> (2015).
- Wang, Y. et al. Exposure to PM<sub>2.5</sub> aggravates Parkinson's disease via inhibition of autophagy and mitophagy pathway. *Toxicology* **456**, 152770. <https://doi.org/10.1016/j.tox.2021.152770> (2021).
- Zanobetti, A., Dominici, F., Wang, Y. & Schwartz, J. D. A national case-crossover analysis of the short-term effect of PM<sub>2.5</sub> on hospitalizations and mortality in subjects with diabetes and neurological disorders. *Environ. Health* **13**. <https://doi.org/10.1186/1476-069x-13-38> (2014).
- Lee, H. et al. Short-term air pollution exposure aggravates Parkinson's disease in a population-based cohort. *Sci. Rep.* **7**. <https://doi.org/10.1038/srep44741> (2017).
- Koros, C., Simitsi, A. & Stefanis, L. Genetics of Parkinson's disease: Genotype-phenotype correlations. *Int. Rev. Neurobiol.* **132**, 197–231. <https://doi.org/10.1016/bs.irn.2017.01.009> (2017).
- Polymeropoulos, M. H. et al. Mutation in the alpha-synuclein gene identified in families with Parkinson's disease. *Science* **276**, 2045–2047. <https://doi.org/10.1126/science.276.5321.2045> (1997).
- Valente, E. M. et al. Hereditary early-onset Parkinson's disease caused by mutations in PINK1. *Science* **304**, 1158–1160. <https://doi.org/10.1126/science.1096284> (2004).
- Kim, J.-H. et al. DJ-1 facilitates the interaction between STAT1 and its phosphatase, SHP-1, in brain microglia and astrocytes: A novel anti-inflammatory function of DJ-1. *Neurobiol. Dis.* **60**, 1–10. <https://doi.org/10.1016/j.nbd.2013.08.007> (2013).
- Ariga, H. et al. Neuroprotective function of DJ-1 in Parkinson's disease. *Oxid. Med. Cell. Longev.* **2013**, 683920. <https://doi.org/10.1155/2013/683920> (2013).
- Shin, S. et al. Effects of ambient air pollution on incident Parkinson's disease in Ontario, 2001 to 2013: A population-based cohort study. *Int. J. Epidemiol.* **47**, 2038–2048. <https://doi.org/10.1093/ije/dyy172> (2018).
- An, R., Ji, M., Yan, H. & Guan, C. Impact of ambient air pollution on obesity: a systematic review. *Int. J. Obes.* **2005**(42), 1112–1126. <https://doi.org/10.1038/s41366-018-0089-y> (2018).
- Strak, M. et al. Associations between lifestyle and air pollution exposure: Potential for confounding in large administrative data cohorts. *Environ. Res.* **156**, 364–373. <https://doi.org/10.1016/j.envres.2017.03.050> (2017).
- Nikolić, M., Stanković, A., Jović, S., Kocić, B. & Bogdanović, D. Effects of air pollution on growth in schoolchildren. *Coll. Antropol.* **38**, 493–497 (2014).
- Su, W. et al. The effect of air pollution and emotional and behavioral problems on preschoolers' overweight and obesity. *Environ. Sci. Pollut. Res. Int.* **29**, 75587–75596. <https://doi.org/10.1007/s11356-022-21144-7> (2022).
- Liu, X.-Q. et al. Neurodevelopmental toxicity induced by PM<sub>2.5</sub> exposure and its possible role in neurodegenerative and mental disorders **42**, 09603271231191436. <https://doi.org/10.1177/09603271231191436> (2023).

23. Kempuraj, D. et al. Brain and peripheral atypical inflammatory mediators potentiate neuroinflammation and neurodegeneration. *Front. Cell. Neurosci.* **11**, 216. <https://doi.org/10.3389/fncel.2017.00216> (2017).
24. Ku, T. et al. Synergistic effects of particulate matter (PM<sub>2.5</sub>) and sulfur dioxide (SO<sub>2</sub>) on neurodegeneration via the microRNA-mediated regulation of tau phosphorylation. *Toxicol. Res.* **6**, 7–16. <https://doi.org/10.1039/c6tx00314a> (2017).
25. Brown, S. J. et al. PINK1 deficiency impairs adult neurogenesis of dopaminergic neurons. *Sci. Rep.* **11**, 6617. <https://doi.org/10.1038/s41598-021-84278-7> (2021).
26. Agnihotri, S. K., Shen, R., Li, J., Gao, X. & Büeler, H. Loss of PINK1 leads to metabolic deficits in adult neural stem cells and impedes differentiation of newborn neurons in the mouse hippocampus. *FASEB J.* **31**, 2839–2853. <https://doi.org/10.1096/fj.201600960RR> (2017).
27. Lee, K. S. et al. Roles of PINK1, mTORC2, and mitochondria in preserving brain tumor-forming stem cells in a noncanonical Notch signaling pathway. *Genes Dev.* **27**, 2642–2647. <https://doi.org/10.1101/gad.225169.113> (2013).
28. Park, J. et al. Drosophila DJ-1 mutants show oxidative stress-sensitive locomotive dysfunction. *Gene* **361**, 133–139. <https://doi.org/10.1016/j.gene.2005.06.040> (2005).
29. Liu, L. L. et al. Loss of DJ-1 function contributes to Parkinson's disease pathogenesis in mice via RACK1-mediated PKC activation and MAO-B upregulation. *Acta Pharmacol. Sin.* **44**, 1948–1961. <https://doi.org/10.1038/s41401-023-01104-8> (2023).
30. Dolgacheva, L. P., Berezhnov, A. V., Fedotova, E. I., Zinchenko, V. P. & Abramov, A. Y. Role of DJ-1 in the mechanism of pathogenesis of Parkinson's disease. *J. Bioenerg. Biomembr.* **51**, 175–188. <https://doi.org/10.1007/s10863-019-09798-4> (2019).
31. Krebiehl, G. et al. Reduced basal autophagy and impaired mitochondrial dynamics due to loss of Parkinson's disease-associated protein DJ-1. *PLoS One* **5**, e9367. <https://doi.org/10.1371/journal.pone.0009367> (2010).
32. Lin, Z. et al. DJ-1 inhibits microglial activation and protects dopaminergic neurons in vitro and in vivo through interacting with microglial p65. *Cell Death Dis.* **12**, 715. <https://doi.org/10.1038/s41419-021-04002-1> (2021).
33. Figge, D. A., Eskow Jaunarajs, K. L. & Standaert, D. G. Dynamic DNA methylation regulates levodopa-induced dyskinesia. *J. Neurosci.* **36**, 6514–6524. <https://doi.org/10.1523/JNEUROSCI.0683-16.2016> (2016).
34. Coppède, F. Genetics and epigenetics of Parkinson's disease. *Sci. World J.* **2012**, 489830. <https://doi.org/10.1100/2012/489830> (2012).
35. Yang, J. et al. CpG demethylation in the neurotoxicity of 1-methyl-4-phenylpyridinium might mediate transcriptional up-regulation of  $\alpha$ -synuclein in SH-SY5Y cells. *Neurosci. Lett.* **659**, 124–132. <https://doi.org/10.1016/j.neulet.2017.08.023> (2017).
36. Tarale, P. et al. Global DNA methylation profiling of manganese-exposed human neuroblastoma SH-SY5Y cells reveals epigenetic alterations in Parkinson's disease-associated genes. *Arch. Toxicol.* **91**, 2629–2641. <https://doi.org/10.1007/s00204-016-1899-0> (2017).
37. Li, H. et al. Short-term exposure to fine particulate air pollution and genome-wide DNA methylation: A randomized, double-blind, crossover trial. *Environ. Int.* **120**, 130–136. <https://doi.org/10.1016/j.envint.2018.07.041> (2018).
38. Plusquin, M. et al. DNA methylation and exposure to ambient air pollution in two prospective cohorts. *Environ. Int.* **108**, 127–136. <https://doi.org/10.1016/j.envint.2017.08.006> (2017).
39. Zhang, L. et al. Fucoidan protects dopaminergic neurons by enhancing the mitochondrial function in a rotenone-induced rat model of Parkinson's disease. *Aging Dis.* **9**, 590–604. <https://doi.org/10.14336/AD.2017.0831> (2018).
40. Guan, L. et al. PM<sub>2.5</sub> inhalation induces intracranial atherosclerosis which may be ameliorated by omega 3 fatty acids. *Oncotarget* **9**, 3765–3778. <https://doi.org/10.18632/oncotarget.23347> (2018).
41. Kawagishi, K. et al. Stereological quantification of olfactory receptor neurons in mice. *Neuroscience* **272**, 29–33. <https://doi.org/10.1016/j.neuroscience.2014.04.050> (2014).
42. Yu, Y. et al. Electroacupuncture produces the sustained motor improvement in 6-hydroxydopamine-lesioned mice. *PLoS One* **11**, e0149111. <https://doi.org/10.1371/journal.pone.0149111> (2016).
43. Liu, A. et al. DNA methylation is involved in pro-inflammatory cytokines expression in T-2 toxin-induced liver injury. *Food Chem. Toxicol.* **132**, 110661. <https://doi.org/10.1016/j.fct.2019.110661> (2019).

## Acknowledgements

This work was supported by the Beijing Tongzhou District Science & Technology Project (KJ2019CX014-30) and (KJ2019CX004-03). The authors thank AiMi Academic Services ([www.aimieditor.com](http://www.aimieditor.com)) for English language editing and review services.

## Author contributions

X.G. and X.W.: study concept and design. X.D.: acquisition of data and wrote the draft. C.C.: made the figure and statistical analysis. L.G.: made a model. All authors contributed to the critical revision of the manuscript and have approved the final version of this review article.

## Declarations

## Competing interests

The authors declare no competing interests.

## Ethics statement

The animal protocols in this study were approved by the Ethics Committee for Animal Experimentation at Capital Medical University (Beijing, China), and all experimental procedures were performed in accordance with the National Institute of Health Guide for the Care and Use of Laboratory Animals (ethical number: 20180712). All methods were performed in accordance with the relevant guidelines and regulations and the ARRIVE guidelines.

## Additional information

**Correspondence** and requests for materials should be addressed to X.W. or X.G.

**Reprints and permissions information** is available at [www.nature.com/reprints](http://www.nature.com/reprints).

**Publisher's note** Springer Nature remains neutral with regard to jurisdictional claims in published maps and institutional affiliations.

**Open Access** This article is licensed under a Creative Commons Attribution-NonCommercial-NoDerivatives 4.0 International License, which permits any non-commercial use, sharing, distribution and reproduction in any medium or format, as long as you give appropriate credit to the original author(s) and the source, provide a link to the Creative Commons licence, and indicate if you modified the licensed material. You do not have permission under this licence to share adapted material derived from this article or parts of it. The images or other third party material in this article are included in the article's Creative Commons licence, unless indicated otherwise in a credit line to the material. If material is not included in the article's Creative Commons licence and your intended use is not permitted by statutory regulation or exceeds the permitted use, you will need to obtain permission directly from the copyright holder. To view a copy of this licence, visit <http://creativecommons.org/licenses/by-nc-nd/4.0/>.

© The Author(s) 2025